

Magnetic transitions and magnetocaloric effect of $\text{Gd}_4\text{Nd}_1\text{Si}_2\text{Ge}_2$

Ronghui Kou^a, Jianrong Gao^{a,*}, Zhihua Nie^b, Yandong Wang^c, Dennis E. Brown^d, Yang Ren^e

^a Key Laboratory of Electromagnetic Processing of Materials (Ministry of Education), Northeastern University, Shenyang 110819, China

^b College of Materials Science and Engineering, Beijing Institute of Technology, Beijing 100124, China

^c State Key Laboratory for Advanced Metals and Materials, University of Science and Technology Beijing, Beijing 100083, China

^d Department of Physics, Northern Illinois University, De Kalb, IL 60115, USA

^e X-ray Science Division, Argonne National Laboratory, Argonne, IL 60439, USA

Abstract

Crystal structure and magnetic properties of the quaternary $\text{Gd}_4\text{Nd}_1\text{Si}_2\text{Ge}_2$ compound were investigated using synchrotron X-ray diffraction and magnetic measurements. The compound crystallized into an orthorhombic structure in the temperature range 200–300 K. In zero field cooling, the compound undergoes a spin reorientation following a ferromagnetic-like transition at 276 K. The spin reorientation is hinted at by nonlinear changes of lattice parameters but is suppressed in a high magnetic field of 6 T. Magnetic measurements revealed a magnetocaloric effect with a high relative cooling power. It is suggested that Nd substitution for Gd enlarges magnetic anisotropy and induces a canted spin structure.

Keywords: Rare earth compound; crystal structure; X-ray diffraction; magnetostriction; magnetocaloric effect

* Corresponding author. E-mail: jgao@mail.neu.edu.cn (J. Gao).

1. Introduction

The $\text{Gd}_5\text{Si}_x\text{Ge}_{4-x}$ system ($x=0-4$) has been intensively investigated because of the discovery of a giant magnetocaloric effect (MCE) at bulk composition with $x = 2$ [1]. The giant MCE is due to a magnetic field-induced transition of first order from a paramagnetic monoclinic structure to a ferromagnetic orthorhombic structure [2]. Both structures are built up by stacking thin Gd_5T_4 slabs ($T = \text{Si}, \text{Ge}$) along the b axis of respective lattices [3]. They have a difference in interslab T–T bonds. Interslab T–T bonds are fully connected in the orthorhombic structure and are half connected in the monoclinic structure. Theoretical and experimental studies [4,5] showed that their ferromagnetism is established through Rudermann-Kittel-Kasuya-Yosida-type (RKKY-type) interactions and dependent on the connection of interslab T–T bonds. Because of such a structure-magnetism interplay, the transition is driven by a gain of the magnetic energy against the lattice strain energy [6]. Apart from a magnetic entropy change, the transition induces a lattice entropy change. The latter is even larger than the former [7]. A recent study showed that a short-range chemical order of Ge atoms in the monoclinic lattice plays a critical role in inducing the giant MCE [8]. This finding explains why the giant MCE can be tuned by annealing as-cast material or by choosing Ge-rich bulk composition [9,10].

Effects of chemical substitutions for T or Gd atoms have been studied for fundamental and technical interest [11,12]. Substitutions of T atoms can strengthen or weaken the interslab T–T bonds allowing for tuning of magnetism and the giant MCE [13,14]. Substitutions of Gd atoms by other rare earth atoms also have significant effects on the crystal structure and magnetism [15]. Heavy rare earth substitutions stabilize the monoclinic lattice at a lower temperature [16]. Then a field-driven transition induces a similar MCE. In contrast, light rare earth substitutions often destabilize the monoclinic

structure and favor a canted spin structure [17,18]. Such effects of light rare earth substitutions are not fully understood yet. Apart from a size difference between rare earth atoms, a difference in the electronic structure can be critical. It was shown recently that a charge transfer of $5d$ electrons from Gd to Nd causes changes of the electronic and the magnetic structure of Nd-substituted Gd_5Si_4 depending on substitution level [19]. Two earlier studies showed that $\text{Nd}_5\text{Si}_2\text{Ge}_2$ and $\text{Nd}_5\text{Si}_{2.4}\text{Ge}_{1.6}$ crystallized into a $\text{Gd}_5\text{Si}_2\text{Ge}_2$ -type monoclinic structure [20,21]. Those observations suggested that the giant MCE of $\text{Gd}_5\text{Si}_2\text{Ge}_2$ might be preserved after a Nd substitution for Gd. Uthaman et al. [22] found that the monoclinic lattice is stabilized at a low substitution level only whereas an orthorhombic lattice is formed at a high substitution level leading to an ordinary MCE. Such effects of Nd substitutions appear similar to those of Ge substitutions for Si [10]. It is an open question whether ferromagnetism of $\text{Gd}_5\text{Si}_2\text{Ge}_2$ is modified by Nd substitutions. To answer this question, we carried out temperature-dependent synchrotron X-ray diffraction and magnetic measurements on the $\text{Gd}_4\text{Nd}_1\text{Si}_2\text{Ge}_2$ compound. Our results suggested the formation of a canted spin structure and a spin reorientation transition due to a high-level Nd substitution.

2. Experimental

Button-sized ingots of bulk $\text{Gd}_4\text{Nd}_1\text{Si}_2\text{Ge}_2$ composition were prepared by arc-melting elements of Gd (99.9% purity), Si (99.99% purity) and Ge (99.999% purity) under protection of a Ti-gettered argon atmosphere of pure argon. In arc-melting, Gd and Nd had to be melted first because of semiconducting nature of solid Si. A high arc current was chosen because of a high melting temperature of the bulk composition. For such reasons, Gd and Nd had mass losses. An excess mass of 10% was added for each rare earth element to compensate for their losses. Raw materials were melted in a water-

cooled hearth several times for bulk homogeneity. Grain morphology and microsegregation of arc-melted ingots were examined using scanning electron microscope (SEM). Elemental concentrations of grains were analyzed using energy dispersive spectrometry (EDS). Small pieces were cut from the ingots and milled into powders for measurements described below.

Differential scanning calorimetric (DSC) measurements were carried out using a QA100 calorimeter supplied by TA instrument at a cooling/warming rate of 10 K min^{-1} . Magnetic measurements were carried out using a superconducting quantum interference device magnetometer. Magnetization of a powder sample was measured in a d.c. magnetic field of 0.02 T in the temperature range 10–380 K and also in a d.c. magnetic field of 2 T in the temperature range 170–330 K. The Curie temperature of the sample, T_C , was determined as a temperature, at which the temperature derivative of magnetization reached a negative maximum. Isothermal magnetization measurements were carried out in d.c. magnetic fields up to 2 T at temperatures close to the T_C . High-energy X-ray diffraction (HEXRD) measurements were carried out on a powder sample at the beamline 11-ID-C of the Advanced Photon Source, Argonne National Laboratory. X-rays used had a wavelength of $\lambda = 0.1078 \text{ \AA}$ and a photon energy of 115 keV. The sample was held at every 10 K in zero-field and field cooling from 290 K down to 200 K. In field cooling, a d.c. magnetic field of 6 T was excited using a superconducting magnet with split coils and held constant. Diffracted X-ray intensities were detected in the forward scattering direction using a two-dimensional amorphous Si detector with a pixel resolution of $200 \times 200 \text{ \mu m}$. More details of the experimental set-up can be found elsewhere [23,24]. After the HEXRD measurements, X-ray intensities were integrated along Debye rings using the software Fit 2D. The sample-to-detector distance was about 1.8 m and further calibrated using a standard

CeO₂ powder sample. Crystal structure, lattice parameters and bond lengths of the sample were determined by Rietveld refinement using the General Structural Analysis Software (GSAS).

3. Results

3.1 SEM investigation

The SEM investigation revealed that grains on the surface of arc-melted ingots were grown into a faceted morphology. Examination of those grains at high magnification unveiled a high density of thin lines. The lines were well seen in secondary electron imaging condition but were less discernible in back-scattered electron imaging condition. Such observations are in good agreement with earlier studies of R₅Si_xGe_{4-x} compounds (R= rare earth) [25]. There are no apparent segregations in intergranular regions. EDS measurements determined that concentrations of Gd and Nd of individual grains are close to their nominal values within experimental errors of ± 2 at.%, suggesting that mass losses in arc-melting were well compensated for. Determined Si and Ge concentrations of the grains had a large scatter due to a channeling effect of incident electrons. Despite the scatter, determined ratios of R over T concentrations are close to 5:4.

3.2 Calorimetric and magnetic measurements

Fig. 1 shows DSC curves of a sample. In a cooling run, an endothermic flow was observed in the temperature range 220–263 K. In a warming run, an exothermic flow was observed in the temperature range 212–272 K. These heat flows are abnormal and suggest a thermally induced transition. The transition appears reversible but has a sluggish kinetics. The mean transition temperature was determined to be 241.5 K and 242 K in cooling and warming, respectively. A difference of 0.5 K is attributed to a high

sweeping rate of 10 K min^{-1} . Thus, the transition is supposed to be of second order.

Fig. 2 shows temperature-dependent magnetization of a sample. A ferromagnetic-like transition was observed at a Curie temperature of $T_C = 276 \text{ K}$ and 279 K during cooling in a low and a medium magnetic field of 0.02 and 2 T , respectively. The transition shows a negligible thermal hysteresis, suggesting a second order. The T_C is about 34 K higher than the mean transition temperature determined by the DSC measurements. This large difference suggests that the ferromagnetic-like transition is not the transition seen in the DSC curves. A third transition was observed at a temperature of about 100 K . It caused an additional rise of magnetization but the rise is smaller than that observed at the T_C . The data of magnetization show thermomagnetic irreversibility in the temperature range $100\text{--}273 \text{ K}$. As seen in Fig. 2a, magnetization in the low field warming is lower than in the low field cooling. This irreversibility can be attributed to pinning of thin domain walls at crystal defects [26]. It is not discernible in warming under the magnetic field of 2 T (see Fig. 2b), suggesting depinning of thin domain walls. Paramagnetic susceptibility of the sample showed an anomaly in the low field measurements. As shown in Fig. 3a, the reciprocal paramagnetic susceptibility in the temperature range $279\text{--}294 \text{ K}$ had positive deviations from a high-temperature Curie-Weiss law. The deviations are due to a two-staged dependence of the reciprocal paramagnetic susceptibility on temperature (see Fig. 3b). Opposite deviations were observed for the reciprocal paramagnetic susceptibility of $\text{Gd}_5\text{Si}_2\text{Ge}_2$ and $\text{Tb}_5\text{Si}_2\text{Ge}_2$ and attributed to short-range ferromagnetic interactions (known as Griffiths phase) [27,28]. Thus, the positive deviations can be attributed to short-range antiferromagnetic interactions in the paramagnetic state of the sample. The deviations were suppressed in thermomagnetic cycles in the medium magnetic field of 2 T (see Figs. 3c and 3d). Such a field effect is similar to that on the Griffiths phase [27,28] and thus, supports the hypothesis of the

origin of the positive deviations.

As shown in Fig. 4a, isothermal magnetization of the sample has a nonlinear field dependence at a few temperatures above the T_C . This nonlinear dependence confirms the anomaly of the paramagnetic susceptibility. As temperature decreases to the T_C or below, isothermal magnetization of the sample showed a steep rise suggesting a field-driven ferromagnetic-like transition. Isothermal magnetization is not saturated at the maximum magnetic field of 2 T. This observation is in good agreement with thermomagnetic measurements and suggests a high magnetic anisotropy in the crystal lattice of the sample (see Fig. 2). Integration of the isothermal magnetization using the Maxwell relationship [29] reveals a MCE near the room temperature. As shown in Fig. 4b, the MCE gives an absolute maximum of the total entropy change of $3.58 \text{ J kg}^{-1} \text{ K}^{-1}$ at a magnetic field change 0–2 T. This absolute maximum is smaller than a value of 5.0 and $14.7 \text{ J kg}^{-1} \text{ K}^{-1}$ reported for pure Gd and the monoclinic $\text{Gd}_5\text{Si}_2\text{Ge}_2$, respectively [1]. However, it is larger than a value of $3.2 \text{ J kg}^{-1} \text{ K}^{-1}$ observed for $\text{Gd}_{4.8}\text{Nd}_{0.2}\text{Si}_2\text{Ge}_2$ [22] and $\text{Gd}_4\text{Nd}_1\text{Si}_4$ [19], suggesting an improvement of the MCE. As shown in Fig. 4b, the MCE of the sample is broadened over temperature relative to that of $\text{Gd}_4\text{Nd}_1\text{Si}_4$. The broadening is more significant at temperatures below the T_C than above the T_C . Because of this broadening, the MCE of the sample has a higher relative cooling power (104 J kg^{-1} vs 93 J kg^{-1}).

3.3 HEXRD measurements

The crystal structure of the sample was determined by Rietveld refinement. As shown in Fig. 5, the sample crystallized into an orthorhombic structure at 290 K and 200 K. This structure is similar to that determined for $\text{Gd}_{4.8}\text{Nd}_{0.2}\text{Si}_2\text{Ge}_2$ [22]. Impurities phases such as Gd_5Si_3 and $\text{Gd}_5\text{Si}_2\text{Ge}_2$ of a monoclinic structure are not suggested by the Rietveld refinement. An assumption of a coexistence of two phases with similar

orthorhombic structures is neither supported by the Rietveld refinement, confirming that the sample has a good chemical homogeneity. The orthorhombic structure remains stable after a high magnetic field of 6 T is applied. However, determined lattice parameters of the sample show variations with temperature and magnetic field. In zero field cooling, the lattice parameters show nonlinear changes at intermediate temperatures in contrast to linear changes at a low and a high temperature end. The changes are anisotropic. As shown in Fig. 6, the parameters a and c and the lattice volume V are reduced during cooling from 270 K to 240 K whereas the parameter b is increased. Such nonlinear changes of the lattice parameters suggest that the sample experiences a transition of second order. The starting and ending temperatures of this transition are close to those of the transition observed by the DSC measurements. Thus, they are assumed to be the same transition. As shown in Fig. 2, magnetization of the sample did not show any change at this transition. Then the transition is identified as a spin reorientation transition following Zou's study of $\text{Tb}_5\text{Si}_{2.2}\text{Ge}_{1.8}$ [30]. The lattice parameters of the sample show temperature-dependent magnetostriction in a high magnetic field of 6 T. The magnetostriction is larger in the paramagnetic region ($T > T_C$) than in the magnetically ordered region. The magnetostriction is anisotropic as usual. While it has a positive sign along the b axis, it has a negative sign along other axes. Because the field-induced changes of the lattice parameters are opposite to those observed in the zero field cooling, it is concluded that the spin reorientation transition is suppressed by the high magnetic field of 6 T. This high field effect suggests that the spin reorientation transition is driven by a gain of the magnetic exchange energy against the thermally induced lattice strains.

Bond lengths and diffraction intensities of the sample also show significant variations with temperature and magnetic field. As shown in Fig. 7, lengths of intraslab and

interslab T–T bonds show similar changes with decreasing temperature. In contrast, lengths of intraslab R–T bonds (R=Gd, Nd) show opposite changes relative to lengths of interslab R–T bonds. The temperature dependence of interslab R–T bonds follows that of the lattice volume change well. This result suggests that the changes of the lattice volume are overwhelmingly controlled by the changes of lengths of intraslab R–T bonds. In field cooling, bond lengths and the lattice volume show linear contractions with decreasing temperature except for the length of interslab R–T bonds. These changes suggest that the high magnetic field modifies lattice strains and their temperature dependences. As shown in Fig. 8, the maximum intensity of few diffraction peaks shows a decreasing tendency in zero field cooling. However, their full width at half maximum shows an increasing tendency. These opposite tendencies suggest that the sample bore thermally induced lattice strains. Those strains can account for the abnormal heat flows observed in the DSC measurements. X-ray diffraction intensities of the sample show much more complex changes in field cooling. The changes of the maximum intensity do not follow those of the full width at half maximum. This result suggests that chemical bonds of the sample are subjected to rotations in addition to elongations or contractions. The determination of the rotations means that the sample has a canted spin structure. Then it is suggested that the magnetic transition observed around 100 K can be another spin reorientation transition. However, this hypothesis awaits verification by extended HEXRD measurements.

4. Discussion

The present study determined a spin reorientation transition in $\text{Gd}_4\text{Nd}_1\text{Si}_2\text{Ge}_2$ and its suppression by a high magnetic field. Although a spin reorientation was observed in $\text{Tb}_5\text{Si}_{2.2}\text{Ge}_{1.8}$ [30], it is rarely observed in the $\text{Gd}_5\text{Si}_x\text{Ge}_{4-x}$ system. Its occurrence in the

title compound is exclusively attributed to the Nd substitution for Gd. We discuss below the microscopic origin of it and its relation to the MCE of the sample.

The paramagnetic anomaly provided a clue for the origin of the spin reorientation. As explained in Section 3.2, the anomaly is the sign of short-range antiferromagnetic interactions. In literature, antiferromagnetic interactions were known for Gd_5Ge_4 and $\text{Gd}_5\text{Si}_{0.5}\text{Ge}_{3.5}$ [31,32]. Unlike the title compound, those compounds crystallize into a Sm_5Ge_4 -type orthorhombic structure, where their interslab R–T bonds fully or half disconnected. This structural difference suggests that the short-range antiferromagnetic interactions in the title compound may not be due to interslab RKKY interactions, but due to intraslab RKKY interactions. Such an assumption is reasonable because similar interactions are established between $4f$ spins of Nd and Gd atoms in the orthorhombic lattice of the $\text{Gd}_{2.5}\text{Nd}_{2.5}\text{Si}_4$ compound due to a charge transfer of $5d$ electrons [19]. The establishment of antiferromagnetic interactions at a lower level of Nd substitution for Gd is understood because Ge atoms can help enlarge interatomic distances between R and T atoms. Assuming that the short-range antiferromagnetic interactions are thermally stable and extended to a long range, the ferromagnetic-like transition at the T_C can be attributed to ferromagnetic ordering of $4f$ spins along the b axis of the orthorhombic lattice through interslab RKKY interactions. Under this assumption, the transition should be specified as a ferrimagnetic transition. Once this transition occurs, it may inversely impose an influence on the intraslab antiferromagnetic interactions. This influence is crucial to the formation of the canted spin structure and provides a strong condition for the spin reorientation. The occurrence of the spin reorientation relies on magnetic anisotropy. In the ferromagnetic lattice of $\text{Gd}_5\text{Si}_2\text{Ge}_2$, a magnetic anisotropy is given by a small difference between the strength of interslab and intraslab RKKY interactions [4]. This anisotropy is supposed to be enlarged upon the Nd

substitution for Gd. On one hand, Nd atoms have a strong single-ion anisotropy [33] and thus, their substitution for Gd atoms can increase the anisotropy of magnetic ions. On the other hand, Nd atoms are likely to occupy R_3 sites of the lattice as they are in $Gd_4Nd_1Si_4$ [19]. This preferential occupation is supposed to enlarge the difference between the interslab and the interslab RKKY interactions because of smaller 4f moments of Nd atoms than those of Gd atoms. Given a high magnetic anisotropy, a cooling-induced contraction of the lattice changes a balance among the magnetic interaction energy, magnetic anisotropy energy and the lattice strain energy thus triggering the spin reorientation transition. After an external magnetic field is applied, the energy balance is likely to be broken leading to suppression of the spin reorientation and forced magnetostriction. We discuss the origin of the magnetostriction as follows.

The field-induced magnetostriction can be understood in terms of a charge transfer effect as well. It was determined elsewhere [19] that the charge transfer of 5d electrons strengthens the spin-orbital coupling of Nd atoms but weakens that of Gd atoms. As explained above, interslab RKKY interactions are established between Nd atoms preferentially occupying R_3 sites. Thus, magnetization response of the title compound to a magnetic field is higher along the b axis of its lattice than that along other axes. Such an anisotropy of magnetization responses and the field-induced instability of the antiferromagnetic interactions account for anisotropic magnetostriction of the lattice. We emphasize here that the field-induced magnetostriction is a critical reason for the improvement of the magnetocaloric effect of the title compound. As shown in Fig. 6d, the field-induced magnetostriction brings about a reduction of the lattice volume over a wide range of temperature. This volumetric change is supposed to stiffen the crystal lattice and bring about a change of the lattice vibration entropy. The lattice vibration entropy change can be added up to a magnetic entropy change across the field-driven

ferrimagnetic transition, thus leading to the improvement and the broadening of the MCE. Although the field-induced magnetostriction does not lead to a giant MCE, it provides a way of improving the MCE of an ordinary ferromagnet. The previous study on CoMnSi actually provided another example of this possibility [23]. From a technical point of view, the improvement of the MCE by the field-induced magnetostriction can be attractive because it reduces a risk of material cracking over numerous magnetic refrigeration cycles [34].

5. Conclusions

The present results have shown nonlinear changes of lattice parameters and field-induced magnetostriction of $\text{Gd}_4\text{Nd}_1\text{Si}_2\text{Ge}_2$ in zero-field and field cooling, respectively. Such observations have provided evidence for a canted spin structure and a spin reorientation transition following a ferrimagnetic transition. It has been suggested that the Nd substitution for Gd induces intraslab antiferromagnetic interactions and enlarges a magnetic anisotropy of the orthorhombic lattice. The field-induced magnetostriction has been suggested to bring about a broadening of the MCE and an improvement of the relative cooling power compared to that of $\text{Gd}_4\text{Nd}_1\text{Si}_4$. Such a field effect may be useful for improvement of a MCE of other ferromagnets.

Acknowledgements

This work was supported by the National Natural Science Foundation of China [grant number 51831003]; the Ministry of Science and Technology of China [grant number 2012CB619405]. The authors thank Y. Q. Wang, J. Y. Lü, H. Q. Wang, J. Q. Wang and

S. Yang for their help in sample preparation, microscopic examination and magnetic measurements. This research used resources of the Advanced Photon Source, a U.S. Department of Energy (DOE) Office of Science User Facility operated for the DOE Office of Science by Argonne National Laboratory under Contract No. DE-AC02-06CH11357.

References

- [1] V.K. Pecharsky, K.A. Gschneidner Jr., Giant magnetocaloric effect in $\text{Gd}_5(\text{Si}_2\text{Ge}_2)$, Phys. Rev. Lett. 78 (1997) 4494–4497. <https://doi.org/10.1103/PhysRevLett.78.4494>.
- [2] W. Choe, V.K. Pecharsky, A.O. Pecharsky, K.A. Gschneidner Jr., V.G. Young Jr., G.J. Miller, Making and breaking covalent bonds across the magnetic transition in the giant magnetocaloric material $\text{Gd}_5(\text{Si}_2\text{Ge}_2)$, Phys. Rev. Lett. 84 (2000) 4617–4620. <https://doi.org/10.1103/PhysRevLett.84.4617>.
- [3] V.K. Pecharsky, K.A. Gschneidner Jr., Phase relationships and crystallography in the pseudobinary system $\text{Gd}_5\text{Si}_4\text{--Gd}_5\text{Ge}_4$, J. Alloys Compd. 260 (1997) 98–106. [https://doi.org/10.1016/S0925-8388\(97\)00143-6](https://doi.org/10.1016/S0925-8388(97)00143-6).
- [4] D. Paudyal, V.K. Pecharsky, K.A. Gschneidner Jr., B. Harmon, Electron correlation effects on the magnetostructural transition and magnetocaloric effect in $\text{Gd}_5\text{Si}_2\text{Ge}_2$, Phys. Rev. B 73 (2006) 144406. <https://doi.org/10.1103/PhysRevB.73.144406>.
- [5] D. Haskel, Y.B. Lee, B.N. Harmon, Z. Islam, J.C. Lang, G. Srajer, Ya. Mudryk, K.A. Gschneidner Jr., V.K. Pecharsky, Role of Ge in bridging ferromagnetism in the giant magnetocaloric $\text{Gd}_5(\text{Ge}_{1-x}\text{Si}_x)_4$ alloys, Phys. Rev. Lett. 98 (2007) 247205. <https://doi.org/10.1103/PhysRevLett.98.247205>.
- [6] G.H. Rao, Correlation between crystal structure and magnetic properties of $\text{Gd}_5(\text{Si}_x\text{Ge}_{1-x})_4$ compounds. J. Phys.: Condens. Matter 12 (2000) L93–L99. <https://doi.org/10.1088/0953-8984/12/6/105>.
- [7] K.A. Gschneidner Jr, Y. Mudryk, V.K. Pecharsky, On the nature of the magnetocaloric effect of the first order magnetostructural transition, Scrip. Mater. 67 (2012) 572–577. <https://doi.org/10.1016/j.scriptamat.2011.12.042>.
- [8] R.H. Kou, J. Gao, Z.H. Nie, Y.D. Wang, D.E. Brown, Y. Ren. Evidence for a short-

- range chemical order of Ge atoms and its critical role in inducing a giant magnetocaloric effect in $\text{Gd}_5\text{Si}_{1.5}\text{Ge}_{2.5}$, *J. Alloys Compd.* 808 (2019) 151751. <https://doi.org/10.1016/j.hallcom.2019.1517151>.
- [9] A.O. Pecharsky, K. A. Gschneidner Jr., V. K. Pecharsky, The giant magnetocaloric effect of optimally prepared $\text{Gd}_5\text{Si}_2\text{Ge}_2$, *J. Appl. Phys.* 93 (2003) 4722–4728. <https://doi.org/10.1063/1.1558210>.
- [10] V.K. Pecharsky, K.A. Gschneidner Jr., Tunable magnetic regenerator alloys with a giant magnetocaloric effect for magnetic refrigeration from ~ 20 to ~ 290 K, *Appl. Phys. Lett.* 70 (1997) 3299–3301. <https://doi.org/10.1063/1.119206>.
- [11] G.J. Miller, Complex rare-earth tetrelides, $\text{RE}_5(\text{Si}_x\text{Ge}_{1-x})_4$: new materials for magnetic refrigeration and a superb playground for solid state chemistry, *Chem. Soc. Rev.* 35 (2006) 799–813. <https://doi.org/10.1039/B208133B>.
- [12] V. Franco, J.S. Blázquez, J.J. Ipus, J.Y. Law, L.M. Moreno-Ramírez, A. Conde, Magnetocaloric effect: from materials research to refrigeration devices, *Prog. Mater. Sci.* 93 (2018) 112–232. <https://doi.org/10.1016/j.pmatsci.201.10.005>.
- [13] Y. Mozharivskyj, W. Choe, A. O. Pecharsky, G. J. Miller, Phase transformation driven by valence electron concentration: tuning interslab bond distances in $\text{Gd}_5\text{Ga}_x\text{Ge}_{4-x}$, *J. Am. Chem. Soc.* 125 (2003) 15183–15190. <https://doi.org/10.1021/ja037649z>.
- [14] V. Svitly, G. J. Miller, Y. Mozharivskyj, $\text{Gd}_5\text{Si}_{4-x}\text{P}_x$: targeted structural changes through increase in valence electron count, *J. Am. Chem. Soc.* 131 (2009) 2367–2374. <https://doi.org/10.1021/ja8085033>.
- [15] K.A. Gschneidner Jr., V.K. Pecharsky, A.O. Pecharsky, V.V. Ivchenko, E.M. Levin, The nonpareil $\text{R}_5(\text{Si}_x\text{Ge}_{1-x})_4$ phases, *J. Alloys Compd.* 303 (2000) 214–222. [https://doi.org/10.1016/S0925-8388\(00\)00747-7](https://doi.org/10.1016/S0925-8388(00)00747-7).

- [16] L. Morellon, C. Magen, P.A. Algarabel, M.R. Ibarra, C. Ritter, Magnetocaloric effect in $Tb_5(Si_xGe_{1-x})_4$, *Appl. Phys. Lett.* 79 (2001) 1318–1320. <https://doi.org/10.1063/1399007>.
- [17] H.F. Yang, G.H. Rao, G.Y. Liu, Z.W. Ouyang, W.F. Liu, X.M. Feng, W.G. Chu, J.K. Liang, Crystal structure and phase relationships in the pseudobinary system $Nd_5Si_4-Nd_5Ge_4$, *J. Alloys Compd.* 346 (2002) 190–196. [https://doi.org/10.1016/S0925-8388\(02\)00524-8](https://doi.org/10.1016/S0925-8388(02)00524-8).
- [18] Y.C. Wang, H.F. Yang, Q. Huang, L.B. Duan, J.W. Lynn, G.H. Rao, Magnetic and crystal structures of the polymorphic $Pr_5Si_2Ge_2$ compound, *Phys. Rev. B* 76 (2007) 064425. <https://doi.org/10.1113/PhysRevB.76.064425>.
- [19] R.H. Kou, J. Gao, Y. Ren, B. Sanyal, S. Bhandary, S.M. Heald, B. Fisher, C.-J. Sun, Charge transfer-tuned magnetism in Nd-substituted Gd_5Si_4 . *AIP Adv.* 8 (2018) 125219. <https://doi.org/10.1063/1.5081457>.
- [20] C. Magen, L. Morellon, P.A. Algarabel, M.R. Ibarra, C. Ritter, A.O. Pecharsky, K.A. Gschneidner Jr., V.K. Pecharsky, Evidence for a coupled magnetic-crystallographic transformation in $Nd_5(Si_{0.6}Si_{0.4})_4$, *Phys. Rev. B* 70 (2004) 224429. <https://doi.org/10.1103/PhysRevB.70.224429>.
- [21] H.F. Yang, G.H. Rao, G.Y. Liu, Z.W. Ouyang, W.F. Liu, X.M. Feng, W.G. Chu, J.K. Liang, Structure dependence of magnetic properties of $Nd_5Si_{4-x}Ge_x$ ($x = 1.2$ and 2), *Phys. B* 325 (2003) 293–299. [https://doi.org/10.1106/S0921-4526\(02\)01542-9](https://doi.org/10.1106/S0921-4526(02)01542-9).
- [22] B. Uthaman, G.R. Raji, S. Thomas, K.G. Suresh, M.R. Varma, Tuning the structural and magnetocaloric properties of $Gd_5Si_2Ge_2$ with Nd substitution, *J. Appl. Phys.* 117 (2015) 013910. <https://doi.org/10.1063/1.4905544>.
- [23] R.H. Kou, J. Gao, G. Wang, Y.D. Liu, Y.D. Wang, Y. Ren, D.E. Brown, Magnetic

- field-induced changes of lattice parameters and thermal expansion behavior of the CoMnSi compound, *J. Mater. Sci.* 51 (2016) 1896–1902. <https://10.1007/s10853-015-9496-9>.
- [24] Y. Ren, High-energy synchrotron X-ray diffraction and its application to in situ structural phase-transition studies in complex sample environments, *JOM* 64 (2012) 140–149. <https://10.1007/s11837-011-0218-8>.
- [25] L.S. Chumbely, O. Ugurlu, R.W. McCallum, K.W. Dennis, Y. Mudryk, K.A. Gschneidner Jr., V.K. Pecharsky, Linear microstructural features in $R_5(\text{Si,Ge})_4$ -type alloys: difficulties in identification, *Acta Mater.* 56 (2008) 527–536. <https://doi:10.1016/j.actamat.2007.10.009>.
- [26] N.K. Singh, K.G. Suresh, A.K. Nigam, Itinerant electron metamagnetism and magnetocaloric effect in $\text{Dy}(\text{Co,Si})_2$, *Solid State Commun.* 127 (2003) 373–377. [https://doi.org/10.1016/S0028-1098\(03\)00441-1](https://doi.org/10.1016/S0028-1098(03)00441-1).
- [27] Z. W. Ouyang, Griffiths-like behavior in Ge-rich magnetocaloric compounds $\text{Gd}_5(\text{Si}_x\text{Ge}_{1-x})_4$, *J. Appl. Phys.* 108 (2010) 033907. <https://doi.org/10.1063/1.3467800>.
- [28] C. Magen, P.A. Algarabel, L. Morellon, J.P. Araújo, C. Ritter, M.R. Ibarra, A.M. Pereira, J.B. Sousa, Observations of a Griffiths-like phase in the magnetocaloric compound $\text{Tb}_5\text{Si}_2\text{Ge}_2$, *Phys. Rev. Lett.* 96 (2006) 167201. <https://10.1013/PhysRevLett.96.167201>.
- [29] A. M. Tishin, Magnetocaloric effect in strong magnetic fields, *Cryogenics* 30 (1990) 127–136. [https://doi.org/10.1016/0011-2275\(90\)90258-E](https://doi.org/10.1016/0011-2275(90)90258-E).
- [30] M. Zou, Ya. Mudryk, V.K. Pecharsky, K.A. Gschneidner Jr., D.L. Schlage, T.A. Lograsso, Crystallography, anisotropic metamagnetism, and magnetocaloric effect in $\text{Tb}_5\text{Si}_{2.2}\text{Ge}_{1.8}$, *Phys. Rev. B* 75 (2007) 024418.

<https://10.1103/PhysRevB.75.024418>.

- [31] Ya. Madryk, A.P. Holm, K.A. Gschneidner Jr., V.K. Pecharsky, Crystal structure-magnetic property relationship of Gd_5Ge_4 by in situ x-ray powder diffraction, Phys. Rev. B 72(2005) 06442. <https://10.1103/PhysRevB/72.064442>.
- [32] Ya. Mudryk, D. Paudyal, V.K. Pecharsky, K.A. Gschneidner Jr., Magnetostructural transition in $Gd_5Si_{0.5}Ge_{3.5}$: magnetic and X-ray powder diffraction measurements, and theoretical calculations, Phys. Rev. B 77 (2008) 024408. <https://10.1103/PhysRevB.77.024408>.
- [33] Z. W. Ouyang, G. H. Rao, Crystal structures, phase relationships, and magnetic phase transitions of R_5M_4 compounds (R= rare earths, M= Si, Ge), Chin. Phys. B 22.9 (2013) 097501. <https://doi.org/10.1088/1674-1056/22/9/097501>.
- [34] K.A. Gschneidner Jr., V.K. Pecharsky, Thirty years of near room temperature magnetic cooling: where we were today and future prospects, Inter. J. Ref. 31 (2008) 945–961. <https://doi.org/j.ijrefrig.2008.01.004>.

Figures

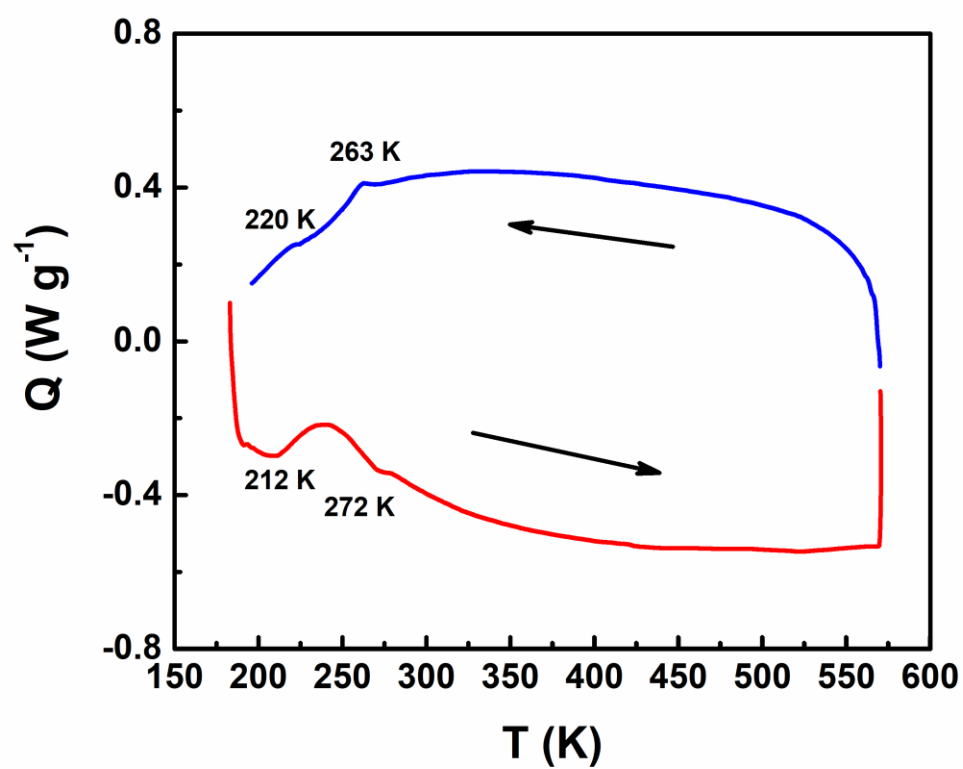


Fig. 1 Heat flows of $\text{Gd}_4\text{Nd}_1\text{Si}_2\text{Ge}_2$ in cooling and warming at a rate of 10 K min^{-1} .

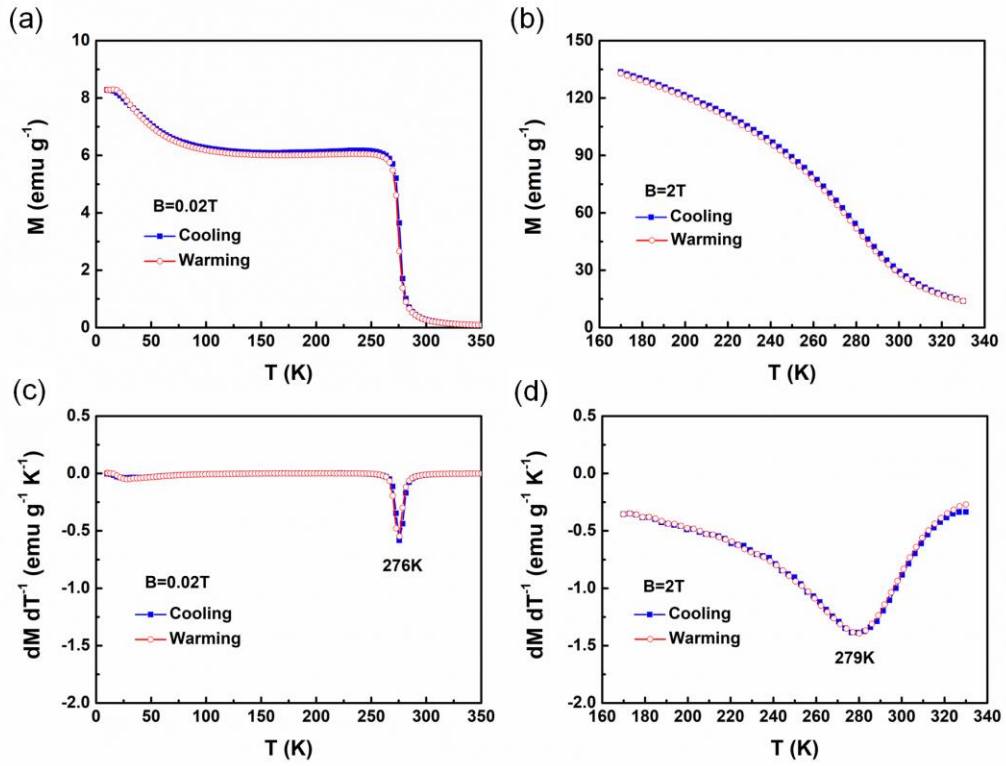


Fig. 2 Temperature dependences of magnetization and its temperature derivative of $Gd_4Nd_1Si_2Ge_2$. (a)(c) 0.02 T (b)(d) 2 T.

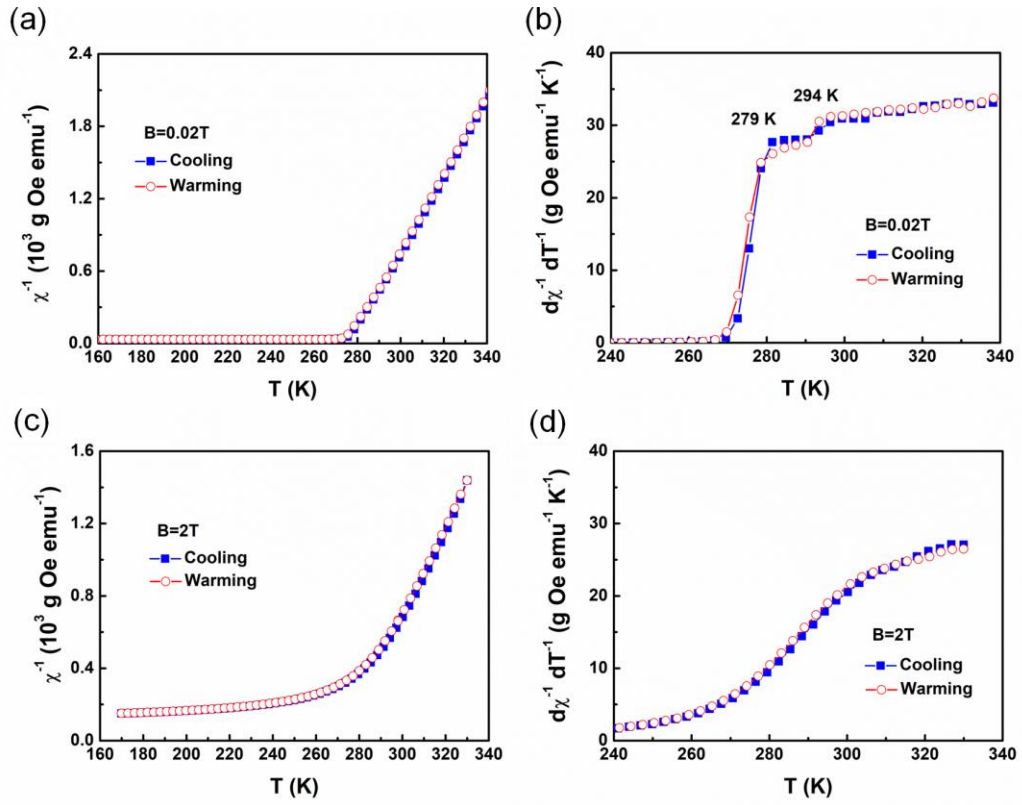


Fig. 3 Temperature dependences of reciprocal paramagnetic susceptibility and its temperature derivative of $Gd_4Nd_1Si_2Ge_2$. (a)(c) 0.02 T (b)(d) 2 T.

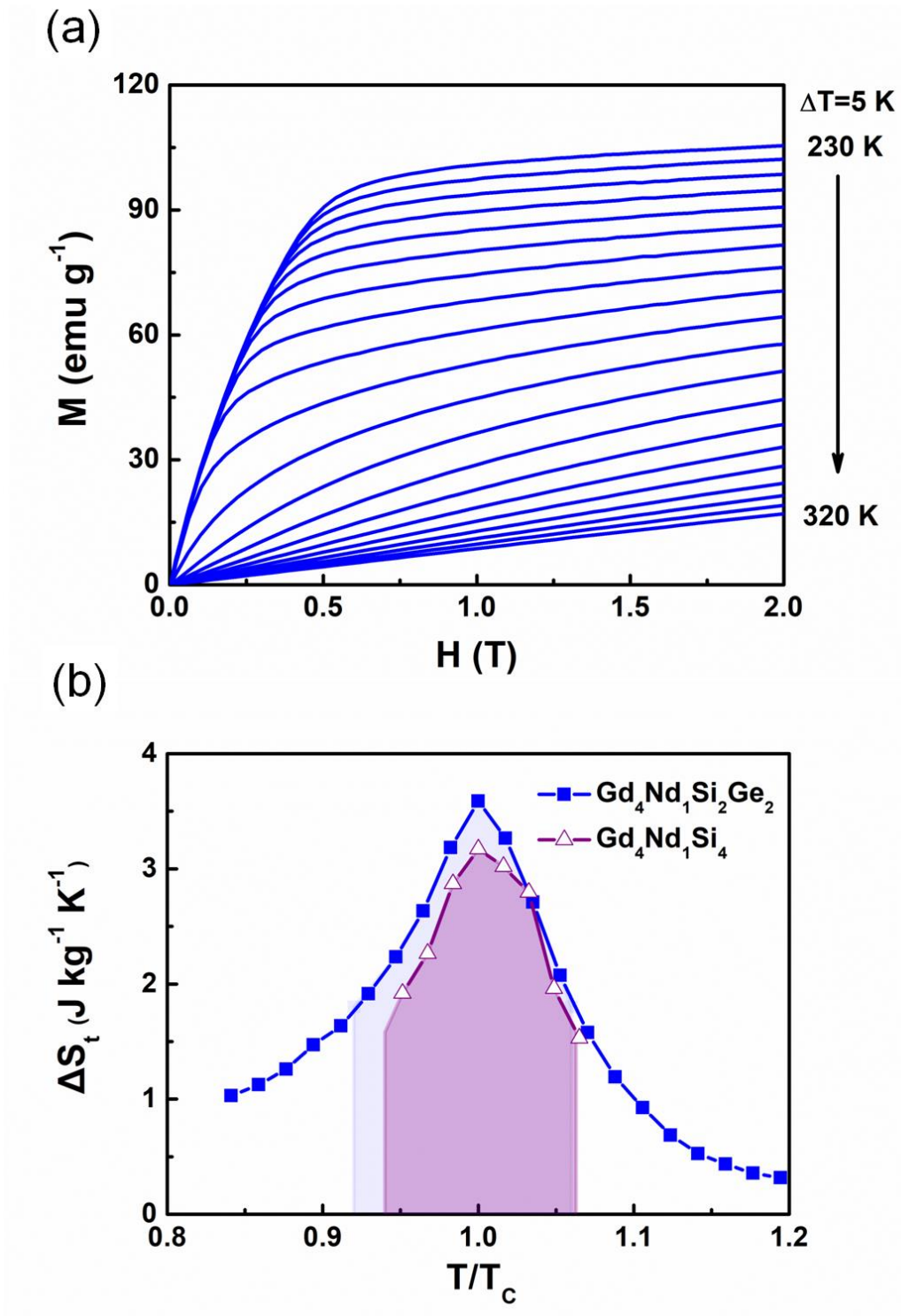


Fig. 4 Temperature dependence of (a) isothermal magnetization and (b) total entropy change of $\text{Gd}_4\text{Nd}_1\text{Si}_2\text{Ge}_2$. Data of $\text{Gd}_4\text{Nd}_1\text{Si}_4$ are taken from Ref. 19 for comparison. In (b), temperature is reduced relative to respective Curie temperature for comparison and a temperature window for determination of relative cooling power is highlighted.

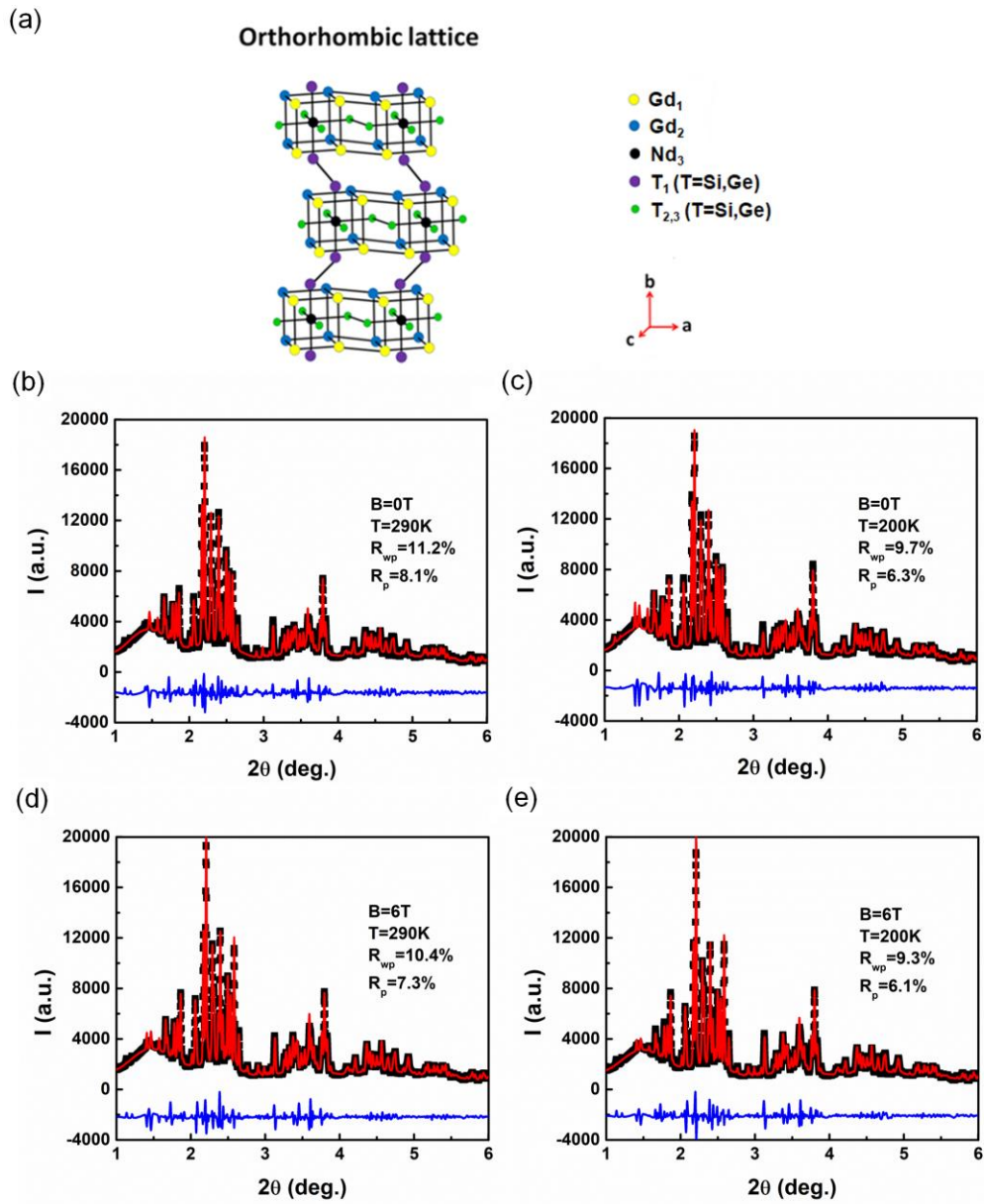


Fig. 5 Rietveld refinement of observed HEXRD patterns of $Gd_4Nd_1Si_2Ge_2$ in zero-field cooling and field cooling. (a) Orthorhombic structure (b) 290 K and 0 T (c) 200 K and 0 T (d) 290 K and 6 T (e) 200 K and 6 T.

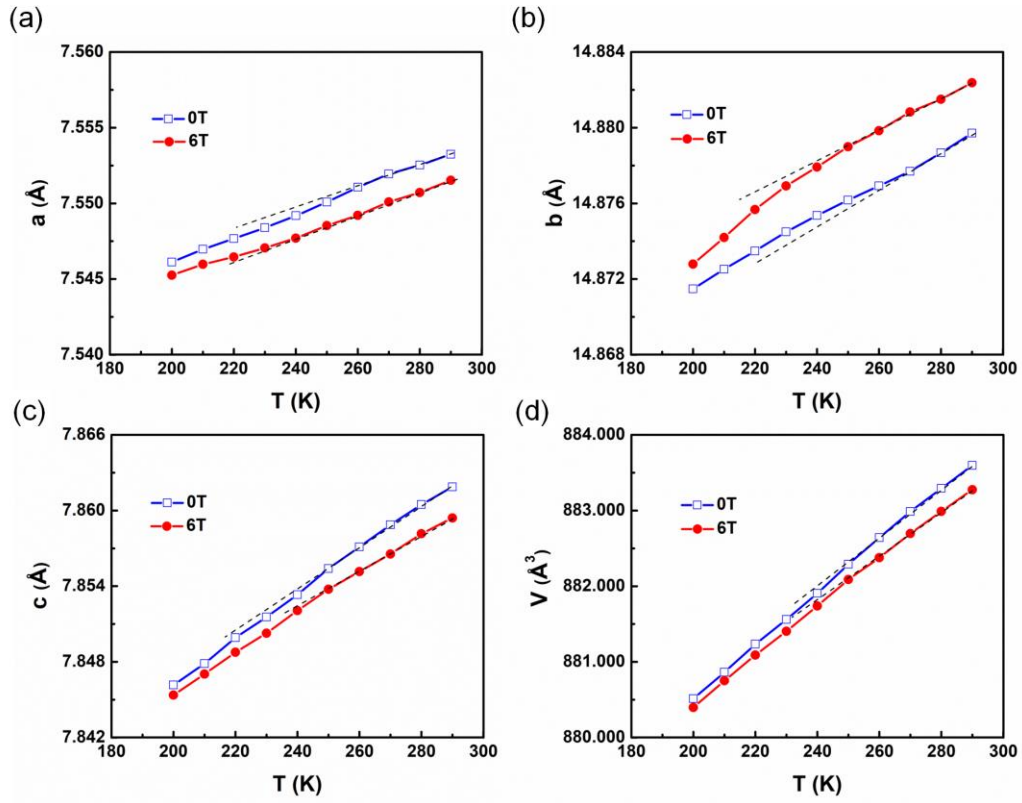


Fig. 6 Temperature dependences of lattice parameters and unit cell volume of $Gd_4Nd_1Si_2Ge_2$ in zero field cooling and field cooling. Dashed lines are draw for eyeguide only. (a)–(c) Lattice parameters (d) unit cell volume.

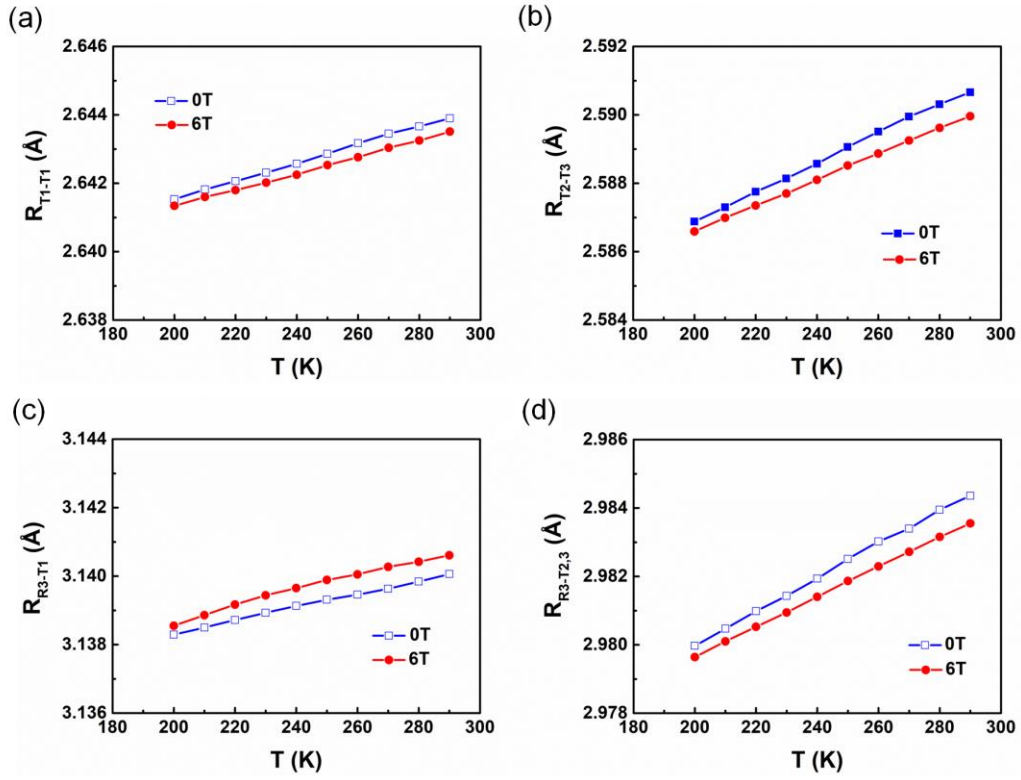


Fig. 7 Temperature dependences of bond lengths of $\text{Gd}_4\text{Nd}_1\text{Si}_2\text{Ge}_2$ in zero field cooling and field cooling. (a) interslab $T-T$ bonds (T_1-T_1) (b) intraslab $T-T$ bonds (T_2-T_3) (c) interslab $R-T$ bonds (R_3-T_1) (d) intraslab $R-T$ bonds ($R_3-T_{2,3}$).

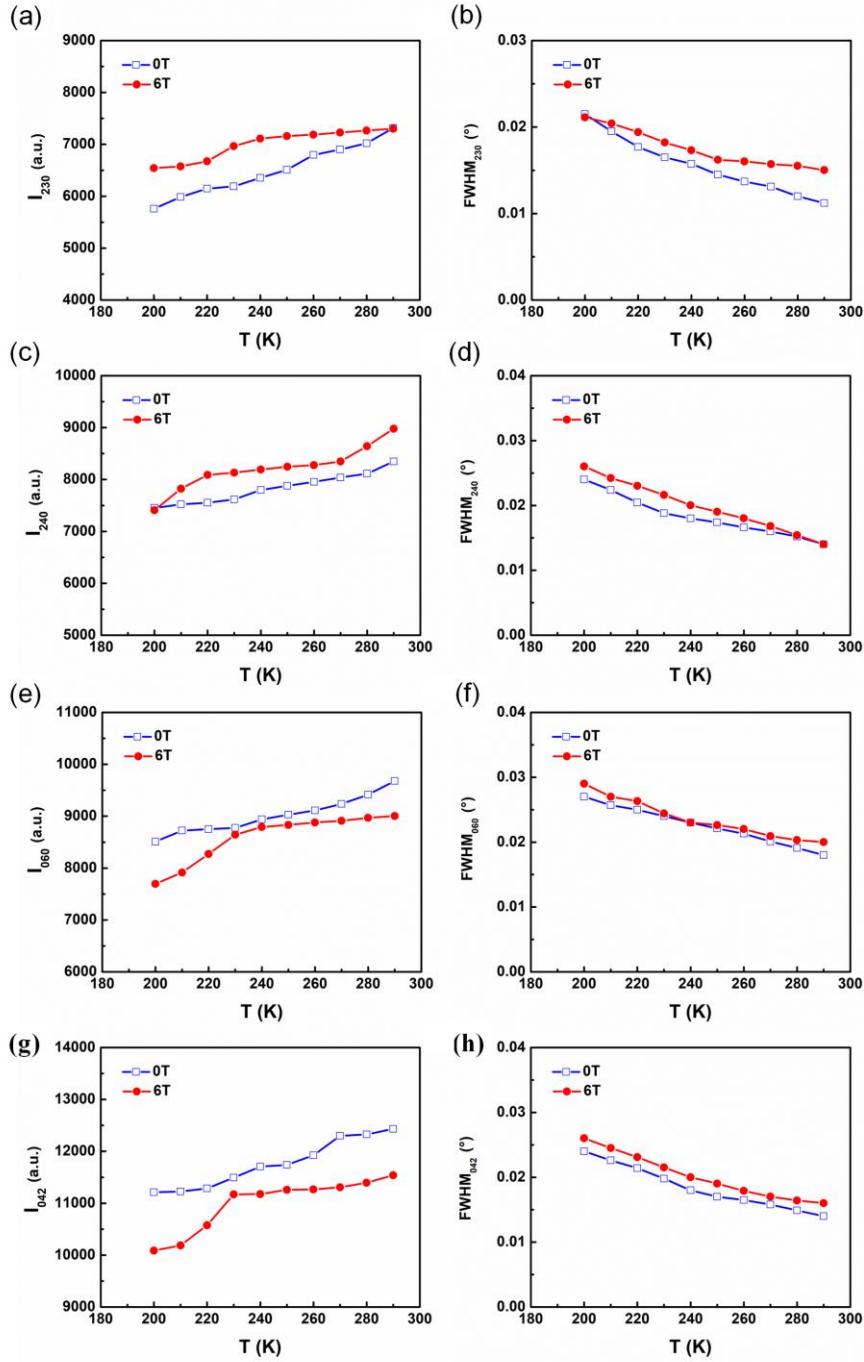


Fig. 8 Temperature dependences of maximum intensity and full width at half maximum of (hkl) diffraction peaks of $Gd_4Nd_1Si_2Ge_2$ in zero field cooling and field cooling. (a)(b) (230) diffraction (c)(d) (040) diffraction (e)(f) (060) diffraction (g)(h) (042) diffraction.